Atp7a determines a hierarchy of copper metabolism essential for notochord development

Bryce A. Mendelsohn,[1,4] Chunyue Yin,[3,4] Stephen L. Johnson,[2] Thomas P. Wilm,[3] Lilianna Solnica-Krezel,[3] and Jonathan D. Gitlin[1,2,*]

[1] Department of Pediatrics
[2] Department of Genetics
Washington University School of Medicine, St. Louis, Missouri 63110
[3] Department of Biological Sciences, Vanderbilt University, Nashville, Tennessee 37235
[4] These authors contributed equally to this work.
*Correspondence: gitlin@kids.wustl.edu

Summary

The critical developmental and genetic requirements of copper metabolism during embryogenesis are unknown. Utilizing a chemical genetic screen in zebrafish, we identified small molecules that perturb copper homeostasis. Our findings reveal a role for copper in notochord formation and demonstrate a hierarchy of copper metabolism within the embryo. To elucidate these observations, we interrogated a genetic screen for embryos phenocopied by copper deficiency, identifying *calamity*, a mutant defective in the zebrafish ortholog of the Menkes disease gene (*atp7a*). Copper metabolism in *calamity* is restored by human ATP7A, and transplantation experiments reveal that *atp7a* functions cell autonomously, findings with important therapeutic implications. The gene dosage of *atp7a* determines the sensitivity to copper deprivation, revealing that the observed developmental hierarchy of copper metabolism is informed by specific genetic factors. Our data provide insight into the developmental pathophysiology of copper metabolism and suggest that suboptimal copper metabolism may contribute to birth defects.

Introduction

Copper is an essential transition metal that plays a critical role in the biochemistry of aerobic organisms. Enzymes utilize the reactivity of this metal to undertake a series of facile electron transfer reactions in a select number of metabolic pathways essential for cellular respiration, iron oxidation, pigment formation, connective-tissue biogenesis, peptide amidation, neurotransmitter biosynthesis, and antioxidant defense (Pena et al., 1999). The signs and symptoms of copper deficiency are the result of impaired function of these cuproenzymes. This reactivity of copper also accounts for the toxicity of this metal when metabolism is perturbed, and for this reason, specific pathways have evolved for the intracellular trafficking and compartmentalization of copper (O'Halloran and Culotta, 2000; Rosenzweig, 2002). The inherited disorders of copper metabolism, Menkes disease and Wilson's disease, underscore both the essential need for copper and the toxicity of this metal, and elucidation of the molecular genetic basis of these diseases has enhanced our understanding of the biochemical mechanisms of copper metabolism (Culotta and Gitlin, 2001; Shim and Harris, 2003).

Considerable clinical and experimental data indicate that copper is an essential nutrient for normal development. In children with Menkes disease, an inability to acquire copper in utero due to inherited loss-of-function mutations in the gene encoding a copper-transport ATPase (*ATP7A*) results in metaphyseal dysplasia, cerebellar degeneration, and severe failure to thrive (Hamza et al., 2001; Voskoboinik and Camakaris, 2002). Similarly, in a variety of mammals, copper deficiency during pregnancy due to either nutrient deprivation or genetic manipulation results in embryo resorption or offspring with severe neurologic impairment and presumed organogenesis defects in multiple tissues including the heart and skeleton (Hamza et al., 2001; Keen et al., 1998). While these data indicate a role for specific transporters and chaperones in supplying copper to the developing fetus (Mercer and Llanos, 2003), the mechanisms and timing of developmental events dependent on copper metabolism remain unknown due to the lack of models affording facile genetic and biochemical analysis during embryogenesis.

We hypothesized that the zebrafish might provide advantages for the analysis of copper metabolism during vertebrate development. The optical clarity and rapid external development of embryos permit detailed characterization of deficient phenotypes from the moment of fertilization. Furthermore, zebrafish embryos have been used in small-molecule screens, permitting the identification of specific developmental phenotypes and the associated genetic pathways (Peterson et al., 2000; Stern et al., 2005; Zon and Peterson, 2005). In this current study, we have utilized chemical genetics combined with a genetic screen (Solnica-Krezel et al., 1994) to elucidate the critical developmental and genetic requirements of copper metabolism during embryogenesis. Our findings provide insight into the developmental pathophysiology of copper metabolism and suggest an experimental approach toward elucidating the biology of gene-nutrient interaction essential for early human development.

Results

Small molecules allow the specific manipulation of copper during development

To obtain precise, temporal control of copper metabolism during development, we determined the minimum copper

concentration in the zebrafish embryo to be 0.5–1.0 μM based on data from oocytes (Riggio et al., 2003). This internal copper pool largely present within the yolk sac is entirely sufficient for embryonic development, as treatment of developing embryos with nonpermeable copper chelators was without effect (data not shown). To identify tools with which to alter this internal copper pool, we employed a chemical genetic screen, reasoning that small molecules interfering with copper metabolism would prevent melanin pigmentation by blocking the activity of tyrosinase, a copper-containing oxidase required for melanin-based pigment in the zebrafish embryo (Rawls et al., 2001). The specificity of this effect was determined by examining these embryos for recovery of tyrosinase activity following the addition of exogenous copper (Figure 1).

Of the small molecules screened (see Table S1 in the Supplemental Data available with this article online), seven of diverse chemical structure prevented melanin pigmentation in a manner entirely reversible by the addition of exogenous copper (Table S2). These small molecules each yielded an identical and striking pleiotropic phenotype, as illustrated in Figure 1, following exposure to neocuproine. Each drug gave the same phenotype at the same time of treatment. Although there were differences in the effectiveness of the compounds as reflected by the doses used, in every case, the identical hierarchy of phenotypes was observed (see below). These small molecules did not affect melanocyte differentiation or migration as determined by in situ hybridization with a melanocyte marker and did not directly inhibit tyrosinase as determined by an in-gel assay (data not shown). Consistent with these experimental findings, review of the literature revealed that each molecule has been associated with copper-chelating activity. Furthermore, none of these compounds has reported teratogenic activity, supporting the concept that the phenotypes observed arise directly from copper deficiency. The identification in this screen of two drugs used in clinical medicine raises the intriguing possibility that unidentified alterations in nutrient metabolism may underlie the therapeutic or toxic mechanisms of additional prescription drugs.

Examination of the copper-deficient phenotype in greater detail was undertaken following treatment of developing embryos with the minimum dose (10 μM) of neocuproine that gave the most robust phenotype. In the zebrafish embryo, the notochord consists of a collection of vacuolated cells surrounded by a sheath, adjacent to the dorsal aorta and the developing floor plate (Figure 2A, left panel). Copper deficiency profoundly altered notochord development, resulting in an undulating structure that contains vacuolated cells but was interrupted by additional tissue structures and surrounded by a thickened floor plate and deformed aorta (Figure 2A, right panel). Further phenotypic analysis of copper-deficient embryos also revealed impaired cartilage and vascular development (Figures 2B and 2C), an absence of hematopoiesis (Figure 2D), and impaired neurogenesis affecting both the midbrain-hindbrain region of the developing brain (Figure 2E) as well as the primary motor neurons (Figure 2F). Interestingly, the hematopoietic defect involved multiple cell lineages (data not shown) analogous to what is observed in mammalian copper deficiency, although the mechanisms of this effect are not well understood. These identical phenotypes were observed with each of the other small molecules identified in this screen and in all cases were prevented by treatment with 25 μM copper chloride dissolved in the egg
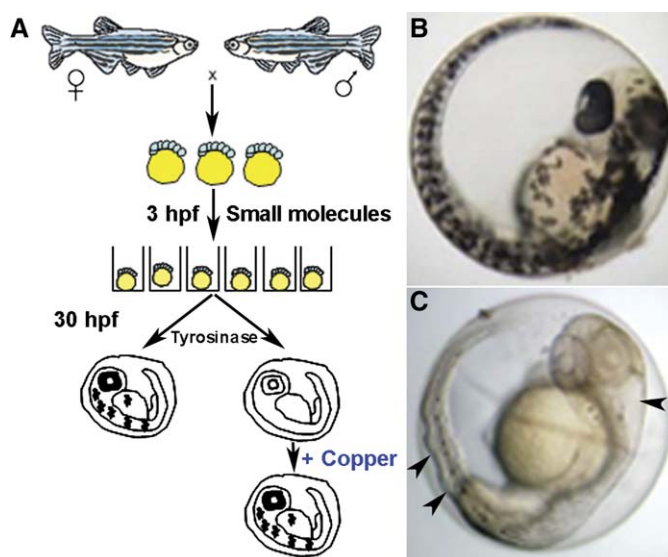

Figure 1. Schematic of the small-molecule screen for drugs perturbing copper metabolism

A) Embryos from wild-type zebrafish were arrayed in a 96-well format and treated with drugs at 5 μM beginning at 3 hr postfertilization (hpf). At 30 hpf, the embryos were assayed for the development of melanin pigment. In a second screen, embryos were again exposed at 3 hpf to drugs that abrogated melanin formation but this time were supplemented with 25 μM CuCl$_2$. In this screen, all drugs that prevented pigmentation in a manner reversible by the addition of exogenous copper were considered as perturbing copper homeostasis.

B and C) As compared to wild-type embryos (**B**), copper-deficient embryos treated with neocuproine (**C**) lacked pigment and displayed a strikingly wavy notochord and enlarged hindbrain ventricle (arrowheads).

water at 5 hr postfertilization (hpf) but not other transition metals including zinc, iron, cobalt, cadmium, and molybdenum (data not shown). These findings also reveal that copper readily enters the embryo from the surrounding water, presumably entering cells through plasma membrane transport, although the route and mechanism of this process are unknown.

These phenotypes of copper deficiency were readily demonstrable following relatively short and early incubation times with the small molecules, suggesting a mechanism of action that permanently renders copper inaccessible to the embryo (Figure 3). Surprisingly, careful observation of embryos treated for brief time periods (Figures 3A–3D) or with submaximal doses of drugs (Figures 3E and 3F) revealed that the threshold of drug for each aspect of the phenotype differed. Thus, while untreated embryos had normal notochords and melanin pigmentation (Figure 3A), treatment for 10 min in 10 μM neocuproine resulted in absence of melanin pigment but a normal notochord (Figure 3B). When such treatment was extended to 20 min, the notochord was clearly abnormal (Figure 3C), and by 60 min, the entire phenotype including the enlarged hindbrain ventricle was observed and did not worsen with longer treatment (Figure 3D). Similarly, embryos incubated continuously starting at 3 hpf in 100 nM neocuproine appeared normal, while treatment with 1 μM drug prevented pigmentation but did not affect the notochord. These findings reveal a hierarchy of copper distribution within the developing embryo that may reflect specific metabolic adaptations based upon the availability of this metal and the essential requirements of each diverse biochemical pathway.
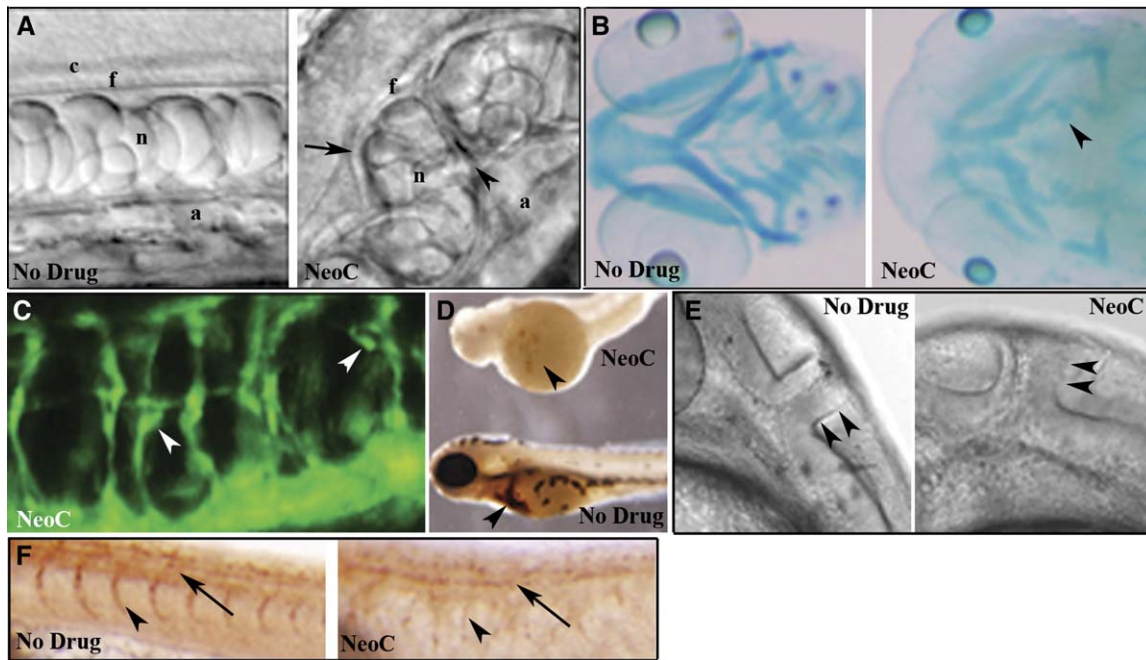
Figure 2. Copper-deficient embryos display a pleiotropic phenotype

DIC image of notochord from a control embryo at 28 hpf (**A**, left) reveals normal development of the central canal (c), floor plate (f), notochord (n), and aorta (a), while a copper-deficient embryo of the same age treated with neocuproine (NeoC) (**A**, right) shows malformations including distorted floor plate (arrow), undulating notochord, additional tissue structures (arrowhead), and displaced aorta. Alcian blue staining of 96 hpf control (**B**, left) and copper-deficient (**B**, right) embryos reveals reduced cartilage formation with compression (arrowhead) and impaired jaw elongation. At 48 hpf, fli1:GFP copper-deficient embryos (**C**) exhibit disorganization of the intersegmental vasculature with microaneurysms (arrowheads). O-dianisidine staining at 72 hpf (**D**) reveals a marked decrease in hematopoiesis (arrowheads) in a copper-deficient embryo (top) compared to control (bottom). DIC image at 32 hpf reveals an abnormal midbrain-hindbrain boundary (arrowheads) in copper-deficient (**E**, right) versus control (**E**, left) embryos. Antibody staining (Znp-1) reveals loss of primary motor neurons (arrow) and associated axons (arrowhead) in copper-deficient (**F**, right) versus control (**F**,left) embryo at 28 hpf.

Copper deficiency phenocopies *calamity*[vu69]

To further understand the molecular genetic basis of such metabolic adaptations in copper homeostasis during embryogenesis, we next interrogated a genetic screen for mutant embryos phenocopied by copper deficiency. Utilizing an ENU-mutagenesis genetic screen, we identified *calamity* (*cal*[vu69]) (Figures 4A and 4B), a recessive lethal mutant with a striking resemblance (particularly in its lack of melanin pigment and wavy notochord) to the chemically induced copper-deficient phenotype. Initial mapping experiments localized *cal* to a region of chromosome 14, 3.5 centimorgans from the *knypek/glypican 4* locus (Topczewski et al., 2001), in proximity to a gene suggested by a BLAST search to encode a copper-transport ATPase. Phylogenetic analysis (Figure 4C) and sequence comparison (Figure S1) indicate that this ATPase identified on chromosome 14 is the ortholog of the human Menkes disease gene, *ATP7A*. A second zebrafish ATPase identified in the BLAST search is the ortholog of the human Wilson's disease gene, *ATP7B* (Figure 4C). As Menkes disease is in part characterized by reduced melanin pigmentation, we considered *atp7a* to be a candidate gene for the locus mutated in *cal*.

Sequence analysis of the zebrafish *atp7a* gene from *cal* mutant embryos identified a mutation creating a cryptic splice acceptor in the intron before exon 9 (Figure 4D), inserting seven additional bases into the mRNA and causing a frameshift and premature stop codon at amino acid 674 of 1482 (Figure 4E). The resulting open reading frame, if translated, would lack all transmembrane and catalytic domains and would therefore be nonfunctional. Restriction digestion of a fragment that was PCR amplified from zebrafish *atp7a* cDNA revealed the absence of wild-type message in *cal* homozygous mutant embryos and a mixture of wild-type and mutant mRNA in their siblings (Figure 4F).

The expression pattern of zebrafish *atp7a* correlates with observed phenotypes

In situ hybridization with a probe to zebrafish *atp7a* revealed ubiquitous and early expression (Figure 5A). A sense-control probe yielded no staining (Figure 5B). Later, significant expression was observed in the developing notochord, with ubiquitous weaker expression in other tissues of the embryo (Figure 5C). Sections revealed *atp7a* expression along the ventricles (Figure 5D) and in the distal notochord (Figure 5E) at 24 hpf. These patterns of expression correlate with the observed *cal* phenotype. A probe to the zebrafish ortholog of the Wilson's disease protein at 5 days postfertilization (dpf) revealed expression in the liver (Figure 5F), consistent with the known expression pattern of *ATP7B* in mammals and demonstrating the conservation of liver-specific expression across metazoans over millions of years of evolution.

Rescue of *calamity* with human ATP7A and assessment of cell autonomy

To confirm the role of *atp7a* deficiency in the *cal* phenotype, synthetic RNA encoding human ATP7A was injected into the zygotes from a *cal* heterozygous cross, significantly suppressing pigmentation and notochord defects in genotypically mutant embryos (Figure 6A). In three separate experiments, 72% of *cal*
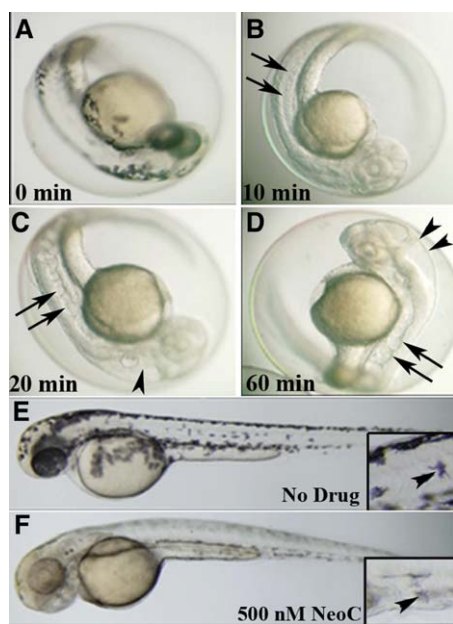
Figure 3. Small-molecule effects are rapid, saturable, and dose and time dependent

Examination of embryo at 48 hpf following no treatment reveals normal melanin pigmentation and notochord (**A**), while treatment with 10 μM neocuproine for 10 min at 3 hpf abrogates melanin pigmentation but does not affect the notochord (arrows) (**B**). Treatment with 10 μM neocuproine for 20 min starting at 3 hpf reveals both abrogated pigmentation, enlarged hindbrain ventricle (arrowhead), and a wavy notochord (arrows) (**C**). Treatment with 10 μM neocuproine for 60 min at 3 hpf does not increase the severity of the pigment, notochord (arrows), or ventricle (arrowheads) phenotype (**D**), indicating that the effect is saturable. Untreated 48 hpf embryo (**E**) shows the normal distribution of melanocytes with melanin pigmentation (inset, arrowhead) and normal notochord, while treatment at 3 hpf with 500 nM neocuproine (one-twentieth of the dose of neocuproine resulting in the complete phenotype) (**F**) impairs only melanin pigmentation (inset, arrowhead).

embryos were entirely rescued by this approach (Figure 6B) while the remainder displayed some normalization of pigmentation and notochord structure. Mechanisms of iron homeostasis have been conserved between humans and zebrafish over millions of years of evolution (Donovan et al., 2000). The restoration of complex developmental phenotypes following expression in the zebrafish of the orthologous human copper transporter similarly demonstrates the functional evolutionary conservation of the genetic and biochemical mechanisms of copper metabolism and provides for a unique experimental system to assess the function of genetic variants of the human Menkes copper transporter.

The availability of a vertebrate model of Menkes disease in an organism where embryonic cell transplantation is possible allowed for a direct analysis of the requirement for *atp7a* in inter- and intracellular copper transport during development. Therefore, we transplanted cells from wild-type donors into *cal* embryos to assess the cell autonomy of the genetic defect. *cal*$^{-/-}$ embryos lack melanin pigmentation (Figure 6C), while in contrast, 35 out of 48 *cal* embryos from three separate transplantation experiments exhibited pigmented donor melanophores or retinal pigment epithelium (Figures 6D–6F). Most interestingly, these transplantation experiments reveal that zebrafish Atp7a acts cell autonomously in melanocytes, suggesting that it is required for proper copper utilization in individual cells and may
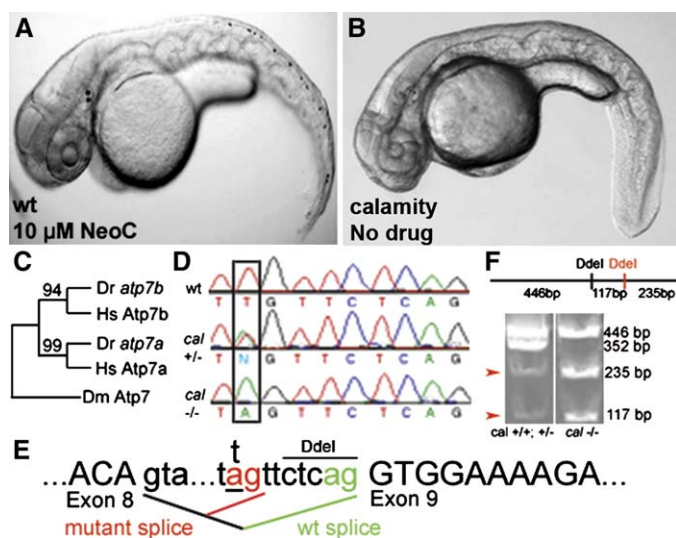

Figure 4. The zebrafish mutant *calamity*^{vu69} is defective in the zebrafish ortholog of the Menkes disease gene and is phenocopied by copper deficiency

A and B) Copper-deficient embryo (**A**) and a *cal* homozygote (**B**) at 48 hpf.
C and D) Phylogeny of copper-transport P type ATPases (**C**) displayed as maximum-likelihood tree with bootstrap values as shown. Aligned nucleotide sequence chromatograms (**D**) from genomic DNA from a portion of the *atp7a* gene from wild-type, *cal* heterozygote, and mutant embryos reveals a T→A transversion (box) in the intron 5′ to exon 9.
E) Analysis of cDNA reverse transcribed from mRNA reveals that this mutation acts as a cryptic splice acceptor causing the insertion of seven nucleotides (TTCTCAG) into the mRNA.
F) Restriction digests of a region amplified from *atp7a* cDNA reveal a novel DdeI site corresponding to the 7 bp insertion at the *cal* locus (arrowheads).

not be essential for copper transport from the yolk sac or within the embryo.

Gene dosage of zebrafish *atp7a* determines the sensitivity to copper deprivation

The developmental hierarchy of copper metabolism observed in embryos treated with variable time or dose exposure to small molecules as well as the cell autonomy observed in the transplantation experiments suggests a complex developmental program of copper metabolism dependent upon both the availability of copper and the function of *atp7a*. To elucidate this complexity of gene-nutrient interaction, we took advantage of our small-molecule screen to precisely modulate copper availability in a specific genetic context. While 100 nM neocuproine did not affect melanin pigmentation in wild-type embryos (Figure 7A), this dose prevented melanin pigment in *cal* heterozygotes (Figure 7B) and worsened the notochord phenotype in *cal* homozygotes (compare Figure 4B and Figure 7C). To more precisely examine this effect, we next utilized an antisense morpholino oligonucleotide (MO) directed against a splice junction in the *atp7a* transcript at a dose that resulted in no apparent phenotype and preserved some wild-type message (Figure S2). Comparison of control MO-injected embryos (Figures 7D–7G) with *atp7a* MO-injected embryos (Figures 7H–7K) at increasing doses of neocuproine revealed that knockdown of *atp7a* strikingly increased the sensitivity of zebrafish embryos to developmental copper deficiency. Most notably, a dose of neocuproine that affected neither pigmentation nor the notochord (Figure 7E) and a dose of *atp7a* MO that yielded no phenotype (Figure 7I)
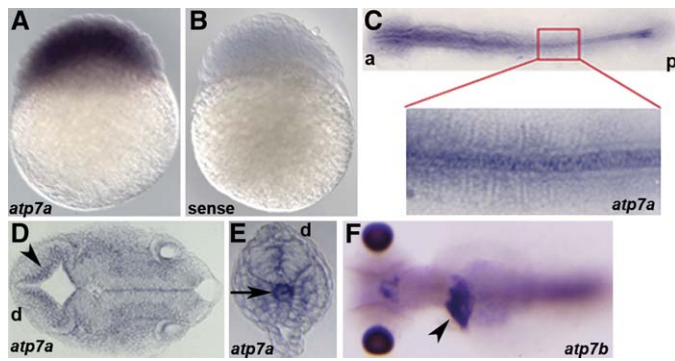
Figure 5. Expression pattern of *atp7a* via in situ hybridization

Anterior (a), posterior (p), and dorsal (d) are as indicated.

A) *atp7a* message is present in all cells at 3 hpf.

B) Staining is specific, as a sense-control probe does not show staining.

C) At 8 somites, *atp7a* is expressed most abundantly in the notochord and is expressed ubiquitously at lower levels.

D and E) Sectioning at 24 hpf reveals staining along the ventricle (**D**) (arrowhead) and in the distal notochord (**E**) (arrow).

F) In situ analysis of *atp7b* reveals expression in the liver (arrowhead) in a 5 dpf embryo as shown in this dorsal view.

Figure 6. Rescue of *cal* with human ATP7A and transplantation experiments

The *calamity* mutant phenotype (**A**) is rescued by injection with synthetic RNA encoding the human Menkes ATPase (**B**). Although *cal* embryos display a complete lack of melanin pigment at 48 hpf (**C**), transplantation of rhodamine-dextran-injected wild-type cells into *cal* embryos (**D**) yields embryos mosaic for pigmented melanophores (arrows). In all cases, the pigmented cells shown here in the retinal epithelium (**E**) correspond to the rhodamine-labeled donor cells as detected by fluorescence for CY3 in this same epithelium (**F**).

caused a severe phenotype when combined (Figure 7J). Taken together, these findings support the hypothesis that the gene dosage of *atp7a* informs the sensitivity of each phenotype to copper deficiency.

Discussion

In this current study, we have utilized chemical genetics combined with a genetic screen to elucidate the critical developmental and genetic requirements of copper metabolism during embryogenesis. Our findings reveal an adaptive hierarchy of copper metabolism as evidenced, for example, by the notochord abnormality, a lethal defect for the developing embryo, that is preferentially preserved when copper availability is limited (Figure 3). Presumably, all such developmental events ultimately depend on the incorporation of copper into specific cuproenzymes, and thus, the mechanisms of this adaptive metabolic hierarchy must arise from differences in either the localization of copper to embryonic structures or the relative affinity of intracellular copper transporters, chaperones, or specific cuproenzymes for this metal (Bertinato and L'Abbe, 2004). This differing threshold of drug for each aspect of the phenotype is not due to differences in tissue penetration, as treatment is initiated prior to any significant differentiation (Figure 3). Our genetic studies suggest that the sensitivity of each phenotype to copper deficiency is determined by gene dosage of *atp7a* (Figure 7), while the transplantation experiments reveal that this sensitivity is cell autonomous such that any cell with sufficient Atp7a for the given availability of copper will produce active cuproenzymes (Figure 6). These observations suggest that in the developing embryo, as copper becomes limiting, tissues expressing higher levels of Atp7a would be advantaged, and in support of this concept, in situ analysis reveals that *atp7a* mRNA is most abundantly expressed in the notochord and ventricles (Figure 5), paralleling the observed hierarchy of sensitivity to copper deficiency.

The notochord is the defining structure of chordates and has essential roles in vertebrate development as a skeletal element
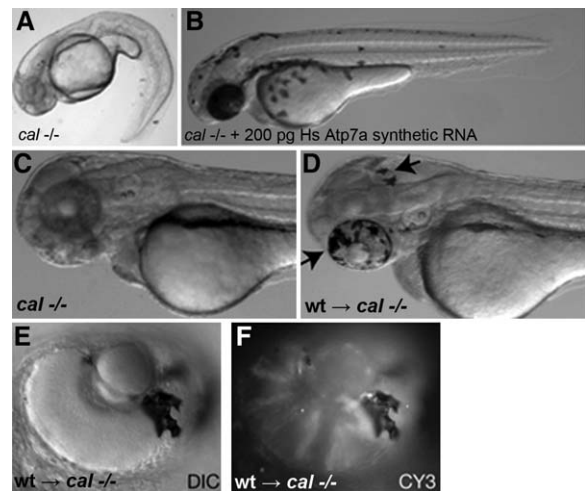
and in the patterning of the surrounding tissues (Stemple, 2005). Our data demonstrate that copper is essential for notochord formation (Figure 2) and raise the interesting possibility that some of the vascular and neurologic abnormalities observed in the offspring of copper-deficient animals and patients with Menkes disease may result from patterning defects secondary to notochord abnormalities. While we have not elucidated the mechanisms of impaired notochord formation in copper deficiency, recent studies in *Xenopus laevis* demonstrate abundant expression of lysyl oxidases within the developing notochord (Geach and Dale, 2005), suggesting that we may have uncovered a role for these cuproenzymes in connective-tissue biosynthesis critical for notochord development (Csiszar, 2001). In mammalian cells, lysyl oxidases are synthesized within the secretory pathway of mesenchymal cells where copper incorporation is dependent upon ATP7A (Voskoboinik and Camakaris, 2002), a finding that would support the hypothesis that the abnormal notochord formation in *cal* (Figure 4) arises from impaired lysyl oxidase activity. In humans, the notochord eventually becomes ossified in regions forming vertebrae and contributes to the nucleus pulposis of the intervertebral discs (Linsenmayer et al., 1986). Our observations that copper is essential for notochord structure raise the intriguing possibility that suboptimal copper availability due either to dietary factors or genetic variation in *ATP7A* or lysyl oxidases during the period of notochord formation or subsequent ossification may contribute to structural birth defects such as congenital scoliosis in which axial skeletal structure is impaired (Blank et al., 1999).

calamity is a newly described zebrafish mutant and a useful model of Menkes disease. Our data demonstrate that *cal* is phenocopied by copper deficiency (Figure 4), a finding to be anticipated in any legitimate model of this disorder. Importantly, while a well-established mammalian model of this disease exists in the *mottled* mouse, the rapid external development of the optically clear zebrafish embryo permits a precise characterization
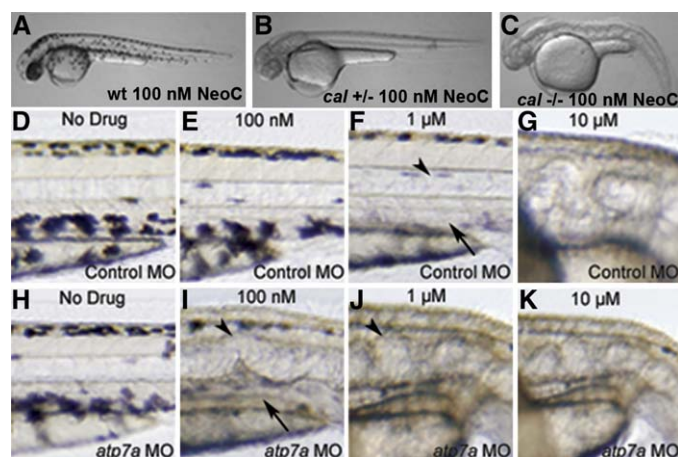
Figure 7. Interaction of *atp7a* dosage and developmental copper deficiency

A and B) Wild-type embryos appear normal in 100 nM neocuproine (**A**); *cal* heterozygotes display loss of all melanin pigment at this same dose (**B**).

C) The pleiotropic phenotype of copper deficiency is observed in all *cal* homozygotes in 100 nM neocuproine.

D–K) Embryos injected with control MO (**D–G**) display a phenotypic dose-response curve in neocuproine of the notochord (arrowheads) and melanin pigment (arrows) that is altered in embryos injected with *atp7a*-targeted MO (**H–K**). All embryos were treated continuously from 3 hpf with the indicated dose of drug.

of the genesis of developmental abnormalities and allows for cellular and genetic manipulations such as transplantation (Figure 6) that are not possible with in utero development. Indeed, our observation of the cell autonomy of this disorder suggests that therapeutic strategies focused upon tissue-specific gene replacement may be a legitimate approach in affected patients. Furthermore, consistent with the observation of cell autonomy, exogenous CuCl$_2$ did not improve the *cal* phenotype. The discovery of a zebrafish model of Menkes disease now permits high-throughput chemical suppression screens (Peterson et al., 2004; Stern et al., 2005) for compounds that restore cuproenzyme function in the setting of a deficiency of the Menkes ATPase, an approach also not possible with the existing murine models. Such drugs would be of immediate clinical relevance.

The relevance of nutrition during development is revealed by recent data highlighting the importance of folate intake before and during pregnancy for preventing neural tube defects (Copp et al., 2003). Despite these observations, the metabolic factors that place specific pregnancies at higher risk remain unknown. Having described the gene-nutrient interactions of copper metabolism and *atp7a* during development, our findings demonstrate the potential of chemical and genetic screens to elucidate the metabolic and genetic interplay of other nutrients that may provide insight into the roles of suboptimal nutrition and genetic variation in human birth defects.

Experimental procedures

Zebrafish maintenance and analysis

SJD and C32 strains were utilized to obtain large numbers of synchronously in vitro-fertilized zebrafish eggs. Embryos were maintained and staged as described previously (Kimmel et al., 1995). The fli1:EGFP transgenic fish are described elsewhere and were generously provided by Brant Weinstein (Motoike et al., 2000). *calamity*[vu69] arose from an ENU-mutagenesis screen for mutants defective in gastrulation and is in the AB/TL background (Solnica-Krezel et al., 1994). Eggs from individual females were collected,

fertilized in vitro with sperm, and allowed to develop at 28.5°C. Synchronized wild-type developing embryos were arrayed as three embryos per well in 96-well plates containing 180 μl of embryo buffer supplemented with methylene blue and ampicillin. Differential interference contrast images (DIC) were obtained using an Olympus IX71 microscope fitted with a Nomarski objective, and images were acquired with a TH4-100 camera and Olympus MicroSuite software. Fluorescently labeled embryos were visualized utilizing a laser scanning confocal microscope (BX61WI FV500; Olympus) equipped with argon 488 and krypton 568 lasers utilizing the 10× objective. Representative fish were imaged using identical confocal settings, and serial *Z* stacks were acquired using a pinhole aperture of 150 μM. Images were collected with FluoView software (Olympus).

Pharmacologic compounds

Approximately 250 small molecules representing all of the major classes of compounds used in clinical medicine as well as a series of known metal chelators were purchased from Sigma, prepared as 5 mg/ml stocks in dimethyl sulfoxide, and then transferred as 20 μl aliquots into individual wells, followed by dilution to ranges from 1 mM to 1 nM for each drug (Table S1). In addition, an array of pharmacologically active small molecules (LOPAC[1280], Sigma) was utilized at 1000-fold dilution for a final concentration of 10 μM. All small molecules were added to the arrayed zebrafish embryos at the 256-cell stage unless otherwise stated, and embryos were examined with an Olympus SZX12 stereomicroscope at 1, 2, and 3 dpf. Phenotypes were recorded when exhibited by each embryo in the well (Peterson et al., 2000). For those drugs identified as potentially interfering with copper homeostasis on the basis of lack of melanin pigmentation at 2 dpf, this analysis was repeated in the presence of 25 μM CuCl$_2$ dissolved in the media.

Immunohistochemistry and in situ hybridization

Embryos raised in phenylthiourea (PTU) were dechorionated and fixed in 4% paraformaldehyde/PBS for 4 hr at room temperature or overnight at 4°C. Embryos were washed in PBS and then water and were permeabilized for 7 min in −20°C acetone, followed by washes in water. The embryos were then blocked for 30 min in PBS/1% DMSO/0.05% Tween 20/10% FBS and incubated overnight in Znp-1 (1:500) antisera (Developmental Studies Hybridoma Bank) in the blocking solution. The antibody was removed and the embryos were washed extensively for 2 hr (Schulte-Merker et al., 1992). Staining was carried out using the VECTASTAIN anti-mouse IgG peroxidase assay (Vector Laboratories) according to manufacturer's instructions. To generate an in situ probe, a 1.6 kb region corresponding to nt 807–2467of the zebrafish *atp7a* cDNA was PCR amplified and used as template to prepare a probe using the DIG-labeling kit (Roche). Various stage embryos were collected and fixed in fresh 4% paraformaldehyde overnight at 4°C, dechorionated, dehydrated with an ascending methanol series (30%, 50%, and 100%), and stored in methanol at −20°C overnight. In situ hybridization was performed as previously described (Thisse et al., 1993).

Alcian blue staining

Embryos at 4 dpf raised in PTU were fixed overnight in 3.7% formaldehyde/PBS, rinsed in PBT (PBS, 0.1% Tween 20), and stained overnight in 0.1% Alcian blue (Sigma) dissolved in 80% ethanol and 20% glacial acetic acid. Embryos were then rehydrated in ethanol:PBT to 100% PBT and cleared in 0.05% trypsin in PBS for 1.5 hr at room temperature, followed by several washes in PBS. Embryos were gradually transferred to 70% glycerol and visualized (Detrich et al., 2004).

Dianisidine staining

Dechorionated 3 dpf embryos were stained at room temperature for 15 min in 2.0 ml o-dianisidine (100 mg/70 ml ethanol), 0.5 ml 0.1 M acetate buffer (pH 4.7), 2.0 ml deionized water, 0.1 ml hydrogen peroxide (30%) followed by rinsing in water (Iuchi and Yamamoto, 1983).

Tyrosinase assay

Ninety-six hours postfertilization embryos were deyolked and lysed in protein extraction buffer (10 mM Tris [pH 7.4], 2% Triton X-100) plus protease inhibitor cocktail (Calbiochem) for 30 min on ice. One hundred micrograms of lysate without β-mercaptoethanol or boiling was run on a 10% SDS gel and assayed for tyrosinase activity as described (Orlow et al., 1993).

calamity sequence analysis

RNA was isolated from 48 hpf *cal* mutant and wild-type siblings using the Trizol method (Invitrogen). First-strand cDNA was generated using the Super-Script III kit (Invitrogen). Gene-specific PCR primers were created using available genomic cDNA sequence and were used to amplify two fragments encompassing the zebrafish *atp7a* open reading frame, which were then cloned into the TA cloning vector pCRII (Invitrogen). The insert was sequenced using internal primers and primers to the flanking vector sequence. A 798 kb PCR product surrounding the 7 bp insertion was amplified from *cal* mutant cDNA and wild-type sibling cDNA, digested with DdeI (NEB) for 3 hr, and run on a 5% polyacrylamide gel. Phylogenetic analysis of zebrafish copper-transport P type ATPases was determined using neighbor-joining and maximum-likelihood methods to construct trees (Mellgren and Johnson, 2005). Accession numbers were as follows: *Homo sapiens* ATP7A, gi:1351993; *Homo sapiens* ATP7B, gi:55957861; *D. rerio* atp7a, gi:70724999; *D. rerio* atp7b, FGENESH00000051998; *D. melanogaster* atp7, gi:45446920.

Cloning of zebrafish *atp7a*

Putative exons encoding the zebrafish *atp7a* gene were found by TBLASTN from the Ensembl zebrafish genome website (http://www.ensembl.org/Danio_rerio/index.html) available as of January 2005. 5′ RACE was used to identify the first exon. The primers used were forward primer 5′-CGAAG AATGGCGCTGAGCAC-3′ and reverse primer 5′-GCTCCAGAGACCCTCAG ACT-3′. These primers were used to amplify from 32 hpf cDNA, and the resulting product was completely sequenced. Alignment of the zebrafish *atp7a* amino acid sequence to human sequences was performed using ClustalW (Thompson et al., 1994).

Morpholino and mRNA injection

A morpholino oligonucleotide (MO) (Nasevicius and Ekker, 2000) 5′-CAAGTC AAGCAGACCTGTTTGCAAT-3′ targeting the splice donor site following exon 16 (Gene Tools) was synthesized, dissolved in Danieau's buffer/phenol red, and injected into one to four cell embryos as 12 ng MO per embryo. A second MO (5′-TTAGTGCTCAGCGCCATTCTTCGTC-3′) targeting the start codon of *atp7a* yielded a similarly increased sensitivity to neocuproine. A standard control MO (Gene Tools) was injected in parallel at the same dose. Synthetic RNA encoding the human Menkes ATPase was generated from pJFM19 using the T7 mMESSAGE mMACHINE kit (Ambion) and polyadenylated with the Poly(A) Tailing Kit (Ambion). Two hundred picograms per embryo was injected.

Transplantation

Rhodamine dextran was injected as a lineage tracer into one-cell wild-type embryos. At the sphere stage, approximately 30 donor cells below the animal pole were transplanted into zygotes of the same age from *cal* heterozygous parents (Lin et al., 2005).

Supplemental data

Supplemental Data include two figures and two tables and can be found with this article online at http://www.cellmetabolism.org/cgi/content/full/4/2/155/DC1/.

References

Bertinato, J., and L'Abbe, M.R. (2004). Maintaining copper homeostasis: regulation of copper-trafficking proteins in response to copper deficiency or overload. J. Nutr. Biochem. *15*, 316–322.

Blank, R.D., Raggio, C.L., Giampietro, P.F., and Camacho, N.P. (1999). A genomic approach to scoliosis pathogenesis. Lupus *8*, 356–360.

Copp, A.J., Greene, N.D., and Murdoch, J.N. (2003). The genetic basis of mammalian neurulation. Nat. Rev. Genet. *4*, 784–793.

Csiszar, K. (2001). Lysyl oxidases: a novel multifunctional amine oxidase family. Prog. Nucleic Acid Res. Mol. Biol. *70*, 1–32.

Culotta, V., and Gitlin, J. (2001). Disorders of copper transport. In The Molecular and Metabolic Basis of Inherited Disease, C. Scriver, A. Beaudet, W. Sly, and D. Valle, eds. (New York: McGraw-Hill), pp. 3105–3136.

H.W. Detrich, M. Westerfield, and L.I. Zon, eds. (2004). The Zebrafish: Cellular and Developmental Biology, Second Edition (Amsterdam: Elsevier Academic Press).

Donovan, A., Brownlie, A., Zhou, Y., Shepard, J., Pratt, S.J., Moynihan, J., Paw, B.H., Drejer, A., Barut, B., Zapata, A., et al. (2000). Positional cloning of zebrafish ferroportin1 identifies a conserved vertebrate iron exporter. Nature *403*, 776–781.

Geach, T.J., and Dale, L. (2005). Members of the lysyl oxidase family are expressed during the development of the frog Xenopus laevis. Differentiation *73*, 414–424.

Hamza, I., Faisst, A., Prohaska, J., Chen, J., Gruss, P., and Gitlin, J.D. (2001). The metallochaperone Atox1 plays a critical role in perinatal copper homeostasis. Proc. Natl. Acad. Sci. USA *98*, 6848–6852.

Iuchi, I., and Yamamoto, M. (1983). Erythropoiesis in the developing rainbow trout, Salmo gairdneri irideus: histochemical and immunochemical detection of erythropoietic organs. J. Exp. Zool. *226*, 409–417.

Keen, C., Uriu-Hare, J., Hawk, S., Jankowski, M., Daston, G., Kwik-Uribe, C., and Rucker, R. (1998). Effect of copper deficiency on prenatal development and pregnancy outcome. Am. J. Clin. Nutr. *67* (*5 Suppl*), 1003S–1011S.

Kimmel, C.B., Ballard, W.W., Kimmel, S.R., Ullmann, B., and Schilling, T.F. (1995). Stages of embryonic development of the zebrafish. Dev. Dyn. *203*, 253–310.

Lin, F., Sepich, D.S., Chen, S., Topczewski, J., Yin, C., Solnica-Krezel, L., and Hamm, H. (2005). Essential roles of G{alpha} 12/13 signaling in distinct cell behaviors driving zebrafish convergence and extension gastrulation movements. J. Cell Biol. *169*, 777–787.

Linsenmayer, T.F., Gibney, E., and Schmid, T.M. (1986). Segmental appearance of type X collagen in the developing avian notochord. Dev. Biol. *113*, 467–473.

Mellgren, E.M., and Johnson, S.L. (2005). *kitb*, a second zebrafish ortholog of mouse *Kit*. Dev. Genes Evol. *215*, 470–477.

Mercer, J.F., and Llanos, R.M. (2003). Molecular and cellular aspects of copper transport in developing mammals. J. Nutr. *133*, 1481S–1484S.

Motoike, T., Loughna, S., Perens, E., Roman, B.L., Liao, W., Chau, T.C., Richardson, C.D., Kawate, T., Kuno, J., Weinstein, B.M., et al. (2000). Universal GFP reporter for the study of vascular development. Genesis *28*, 75–81.

Nasevicius, A., and Ekker, S.C. (2000). Effective targeted gene 'knockdown' in zebrafish. Nat. Genet. *26*, 216–220.

O'Halloran, T.V., and Culotta, V.C. (2000). Metallochaperones, an intracellular shuttle service for metal ions. J. Biol. Chem. *275*, 25057–25060.

Orlow, S.J., Lamoreux, M.L., Pifko-Hirst, S., and Zhou, B.K. (1993). Pathogenesis of the platinum (cp) mutation, a model for oculocutaneous albinism. J. Invest. Dermatol. *101*, 137–140.

Pena, M.M.O., Lee, J., and Thiele, D.J. (1999). A delicate balance: homeostatic control of copper uptake and distribution. J. Nutr. *129*, 1251–1260.

Peterson, R.T., Link, B.A., Dowling, J.E., and Schreiber, S.L. (2000). Small molecule developmental screens reveal the logic and timing of vertebrate development. Proc. Natl. Acad. Sci. USA *97*, 12965–12969.

Peterson, R.T., Shaw, S.Y., Peterson, T.A., Milan, D.J., Zhong, T.P., Schreiber, S.L., MacRae, C.A., and Fishman, M.C. (2004). Chemical

suppression of a genetic mutation in a zebrafish model of aortic coarctation. Nat. Biotechnol. *22*, 595–599.

Rawls, J.F., Mellgren, E.M., and Johnson, S.L. (2001). How the zebrafish gets its stripes. Dev. Biol. *240*, 301–314.

Riggio, M., Filosa, S., Parisi, E., and Scudiero, R. (2003). Changes in zinc, copper and metallothionein contents during oocyte growth and early development of the teleost Danio rerio (zebrafish). Comp. Biochem. Physiol. C Toxicol. Pharmacol. *135*, 191–196.

Rosenzweig, A.C. (2002). Metallochaperones: bind and deliver. Chem. Biol. *9*, 673–677.

Schulte-Merker, S., Ho, R.K., Herrmann, B.G., and Nusslein-Volhard, C. (1992). The protein product of the zebrafish homologue of the mouse T gene is expressed in nuclei of the germ ring and the notochord of the early embryo. Development *116*, 1021–1032.

Shim, H., and Harris, Z.L. (2003). Genetic defects in copper metabolism. J. Nutr. *133*, 1527S–1531S.

Solnica-Krezel, L., Schier, A.F., and Driever, W. (1994). Efficient recovery of ENU-induced mutations from the zebrafish germline. Genetics *136*, 1401–1420.

Stemple, D.L. (2005). Structure and function of the notochord: an essential organ for chordate development. Development *132*, 2503–2512.

Stern, H., Murphey, R., Shepard, J., Amatruda, J., Straub, C., Pfaff, K., Weber, G., Tallarico, J., King, R., and Zon, L. (2005). Small molecules that delay S phase suppress a zebrafish bmyb mutant. Nat. Chem. Biol. *1*, 366–370.

Thisse, C., Thisse, B., Schilling, T.F., and Postlethwait, J.H. (1993). Structure of the zebrafish snail1 gene and its expression in wild-type, spadetail and no tail mutant embryos. Development *119*, 1203–1215.

Thompson, J.D., Higgins, D.G., and Gibson, T.J. (1994). CLUSTAL W: improving the sensitivity of progressive multiple sequence alignment through sequence weighting, position-specific gap penalties and weight matrix choice. Nucleic Acids Res. *22*, 4673–4680.

Topczewski, J., Sepich, D.S., Myers, D.C., Walker, C., Amores, A., Lele, Z., Hammerschmidt, M., Postlethwait, J., and Solnica-Krezel, L. (2001). The zebrafish glypican knypek controls cell polarity during gastrulation movements of convergent extension. Dev. Cell *1*, 251–264.

Voskoboinik, I., and Camakaris, J. (2002). Menkes copper-translocating P-type ATPase (ATP7A): biochemical and cell biology properties, and role in Menkes disease. J. Bioenerg. Biomembr. *34*, 363–371.

Zon, L.I., and Peterson, R.T. (2005). In vivo drug discovery in the zebrafish. Nat. Rev. Drug Discov. *4*, 34–44.

Accession numbers

The coding sequence of zebrafish *atp7a* has been deposited into GenBank with the accession number DQ100352, and its predicted protein translation has been deposited with the accession number AAZ07896.